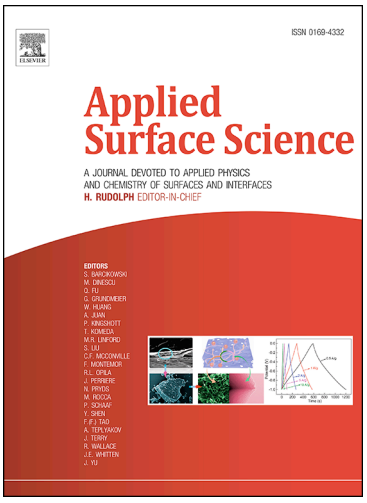

Full Length Article

Carbon black nanospheres modified with Cu (II)-Phthalocyanine for electrochemical determination of Trimethoprim antibiotic

Thais T. Guaraldo, Lorena A. Goulart, Fernando C. Moraes, Marcos R.V. Lanza

PII: S0169-4332(18)32658-8
DOI: https://doi.org/10.1016/j.apsusc.2018.09.226
Reference: APSUSC 40530

To appear in: *Applied Surface Science*

Received Date: 29 May 2018
Revised Date: 25 September 2018
Accepted Date: 26 September 2018

Please cite this article as: T.T. Guaraldo, L.A. Goulart, F.C. Moraes, M.R.V. Lanza, Carbon black nanospheres modified with Cu (II)-Phthalocyanine for electrochemical determination of Trimethoprim antibiotic, *Applied Surface Science* (2018), doi: https://doi.org/10.1016/j.apsusc.2018.09.226

Carbon black nanospheres modified with Cu (II)-Phthalocyanine for electrochemical determination of Trimethoprim antibiotic

Thais T. Guaraldo[1]*, Lorena A. Goulart[1]*, Fernando C. Moraes[2], Marcos R.V. Lanza[1,3*]

[1]São Carlos Institute of Chemistry, University of São Paulo, São Carlos, SP, Brazil
[2]Chemistry Department, Federal University of São Carlos, São Carlos, SP, Brazil
[3]National Institute for Alternative Technologies of Detection, Toxicological Evaluation and Removal of Micropollutants and Radioactives (INCT-DATREM), Institute of Chemistry of Unesp, Araraquara, Brazil

Abstract

This work investigates the electrochemical sensing properties of glassy carbon (GC) electrodes modified with Printex L6 carbon black (PC) and copper (II) phthalocyanine (CuPh) films. Successful incorporation of the CuPh into carbon black was confirmed by FEG-SEM, EDS and TEM analysis. The transition from nanocrystalline graphite to amorphous carbon material could be evidenced for Printex L6 carbon black using Raman analysis. The modified material (CuPh/PC/GC) demonstrated electrocatalytic effect towards TMP detection according to cyclic voltammetric studies. CuPh modification resulted in strong adsorption to carbon black and TMP due to π-π interactions. Scan rate studies proved reactions across the electrode/electrolyte interface progressively change from adsorption to diffusion. The developed method presented linear relationship in the ranges of 0.4 to 1.1 μmol L^{-1} and 1.5 to 6.0 μmol L^{-1} with limit of detection of 0.6 μmol L^{-1} under optimized experimental conditions. The proposed CuPh/PC/GC electrode was effectively employed towards the detection of TMP in natural water samples.

Key words: carbon black, Printex L6, copper phthalocyanine, Trimethoprim determination, environmental samples.

*First co-author: both first and second authors have contributed equally towards the development and drafting of this work.

1 Introduction

Carbon nanomaterials have been extensively applied in electrochemical sensing over the last decade or so. Materials such as single and multi-walled carbon nanotubes (CNTs), graphene, nanodiamond powder, fullerene and carbon nitride are endowed with outstanding properties useful for electrochemical applications. [1–3] Carbon black (CB) is defined as a class of fine-particle powder with different physicochemical properties depending on synthesis conditions. The product is manufactured at relatively lower costs compared to other carbon-based nanomaterials. [4] Apart from elemental carbon, organic and inorganic compounds may also be found on its surface. [4] CB can be industrially manufactured via the oil furnace process which involves the pyrolysis of heavy aromatic petroleum oils at high temperatures. [4] Recently, CB materials have been described as promising sensing materials for the determination of substances in solution. [2,5] CB is endowed with specially distinct features that render it suitable for application in fuel cells, [6] batteries, [7] sensors, [1] hydrogen peroxide electrosynthesis [8,9] and degradation of organic pollutants. [10] Printex L6 carbon (PC) particularly presents a hydrophilic character compared to other CB materials which may facilitate applications in aqueous solutions. To date, few studies have reported the application of CB as sensing material for compounds detection in aqueous systems. [5] For this reason, understanding structural, morphological and electrochemical properties of CB materials would certainly contribute to progress in this field.

Metalloporphyrins and metallophthalocyanines are tetrapyrrolic macrocycles of great interest in chemical, analytical, and photochemical applications. [11] These compounds exhibit great structural similarities and electrocatalytic properties. [12] Furthermore, they are employed in electrochemical sensors due to their photochemical, magnetic, electrochemical and catalytic properties. [13] Mphuthi, *et al.(2017)* defined phthalocyanines and their derivatives as blue-green organic semiconductor materials. These substances belong to the aromatic heterocyclic conjugated molecules family and they are known to be relatively conductive as a result of delocalised *π*-electrons system. The redox properties of metal phthalocyanines (Phs) essentially depend on the interactions and delocalisation of these *π*-systems. [14] Phs are known to have good thermal and chemical stability apart from their capability of changing the metal ion attached to the organic chain which can bring forth unique properties that are conducive to the development of electrochemical sensors. Remarkably, Phs have contributed significantly towards improvements in the performance of CNT-based devices owing largely to their suitable electronic and photoelectronic properties. [14] The functionalisation of CNTs using Phs usually enhances the electrochemical response. Several electrocatalytic and electroanalytic applications of CNTs and phthalocyanines are reported involving O_2 and H_2O_2 electrocatalysis reactions and oxidation reactions of micropollutants as pesticide, herbicide, dye and endocrine disruptor. [15,16] This explains why they are considered promising sensing materials.

Trimethoprim (TMP) is a synthetic antibiotic used for the treatment of several infections (intestinal, urinary and respiratory) in humans and animals,

[17] and for prophylactic purposes [18] acting as dihydrofolate reductase inhibitor (DHFR inhibitor). TMP is commonly associated with sulphonamides with the aim of achieving higher effectiveness of treatment. [18] It can also be found as single-drug formulation. [19] Furthermore, TMP derivatives have been synthesised as a result of antimicrobial resistance [20] posing several risks to human health. [21] Reports in the literature point out that a high percentage (50-70%) of TMP dose is excreted in its pharmacologically active form. [17,22] The toxicity effects of these TMP residues on the aquatic environment especially on the green algae *P. subcapitata* (ErC_{50} 129 mg L^{-1}; ErC_{10} 65 mg L^{-1}) and daphnids (ErC_{50} 100 mg L^{-1}; ErC_{10} 66 mg L^{-1}) have been demonstrated. [23] Accordingly, the relevance of developing new methods for monitoring the residues of this substance in the environment and their hazardous effects needs not be overemphasised [24]. Close monitoring can be conducted either by assisting with medical diagnosis or through environmental remediation practices.

TMP residues have already been determined in human urine, pharmaceutical formulations, natural water and feed samples. Interestingly, liquid chromatography is the most widely reported method for TMP determination. [25,26] Other methods employed towards the determination of this compound such as capillary electrophoresis, [27] spectrophotometry [28] and electroanalysis [29,30] have also been described in the literature. Among the electroanalytical methods, there have been reports about the use of materials such as MIP-graphene-GC [18] and multi-walled CNTs decorated with Prussian blue nanocubes. [22] Usually, chromatographic methods consume large amounts of solvents apart from requiring sample preparation and/or

extraction. Electroanalytical methods use reduced solution volume during analyses, are sensitive, selective, accurate and when compared to liquid chromatography are faster and cheaper. In addition, important information on the electrochemical mechanisms can be obtained as well as analytes determination at submicromolar level [31]. Several materials can be used in the manufacture of electrochemical sensors while the chromatographic columns are generally very specific. CB based materials, could be a cost-effective alternative platform to the expensive CNTs and time-consuming MIP based materials for manufacture of sensors. Besides, simple preparation methods meet the requirements of Green Chemistry.

Thus, in the present work, a glassy carbon electrode was modified with Printex L6 carbon black (PC) and copper phthalocyanine (CuPh/PC/GC) creating a new nanocarbon-based platform to be used in the electrochemical determination of Trimethoprim in natural water samples using square-wave adsorptive anodic stripping voltammetry.

2 Experimental

2.1 CuPh/PC/GC material synthesis

Prior to use, the glassy carbon electrode was carefully polished in alumina (0.05 µm) using a polishing cloth and rinsed in ultrapure water. The electrodes were sonicated in ultrapure water and isopropanol for 5 min each.

Copper (II) phthalocyanine/carbon black (CuPh/PC) dispersion was made according to the procedure previously described by our group. [32] Briefly, PC carbon was dried at 120 ^{o}C for 24 h to enable water removal. Different proportions of CuPh/PC [1:2, 1:4 and 1:6 (wt %)] were then obtained in

the presence of isopropanol. The mixture was kept under magnetic stirring for 1 h. The powder was maintained at 60 ^{o}C for 2 h and at 100 ^{o}C for an extra hour in an oven. Upon drying, the powder was macerated for homogenisation. The same procedure was repeated in the absence of phthalocyanine aiming at obtaining the pure carbon black powder (PC). A dispersion containing only copper phthalocyanine (CuPh) in water was also prepared for comparison purposes.

The glassy carbon electrode surface was modified by casting (20 µL) from the previously prepared dispersions (1.0 mg/mL) containing PC and/or CuPh. Finally, the electrodes were kept and dried for 2h in a dissector so as to obtain the CuPh/PC/GC and PC/GC films.

2.2 Chemicals and solutions

The Printex L6 carbon black sample was purchased from Evonik Brazil while copper (II) phthalocyanine was obtained from Sigma-Aldrich. Trimethoprim (Sigma-Aldrich) stock solutions were prepared on a daily basis in ethanol:water (50:50 - v/v). Sulphuric acid was purchased from Panreac. Phosphate buffer (PBS) solution 0.2 mol L^{-1} (pH 7.0) was prepared using NaH_2PO_4 and Na_2HPO_4. NaOH was used to adjust the pH value. The PBS was chosen for analysis because it has a wide buffering range and composition of polyprotic acids which function as buffers.

All other chemicals used were of analytical grade. All solutions were prepared with ultra-pure water (>18.2 MΩ).

2.3 TMP analysis in natural water

Natural water was collected from a stream in the city of Sao Carlos (Sao Paulo State, Brazil) (coordinates -22.003768S and -47.931165W) located inside Sao Paulo University area 2. The natural river water samples were used as electrolyte for the TMP addition and recovery studies without any kind of pre-treatment. The PBS (pH 7.0) solution was mixed with the natural water (50:50) and spiked with TMP solutions at 5.0 and 10.0 µmol L^{-1} levels. The TMP content was determined by three successive additions of standard stock solution (n=3).

2.4 Materials analysis and characterization

A potentiostat/galvanostat µAutolab (typeIII) was used in all electrochemical measurements controlled by NOVA 1.11 software. The measurements were conducted in a conventional three-electrode cell equipped with glassy carbon electrode (5.0 mm diameter) representing the working electrode, Pt wire being the counter electrode and Ag/AgCl (KCl 3.0 mol L^{-1}) as the reference electrode. Cyclic voltammetry (CV) experiments were carried out within a potential range of 0.3 V to +1.3 V with a scan rate of 50 mV s^{-1}. Square wave voltammetry (SWV) experiments were conducted at 10 Hz of frequency, amplitude of 40 mV, and 5 mV step potential. Other parameters such as conditioning potential and time, which are found to influence the square-wave adsorptive anodic stripping voltammetry (SWAdASV) technique, were studied and optimized (0.6 V and 120 s). Analytical curves were obtained through the addition of aliquots of the TMP standard solutions. The detection limit was calculated considering blank solution deviation (n = 10) times three divided by

the analytical curve slope. The TMP concentration in the analytical curve was determined in triplicate.

Field Emission Gun Scanning electron microscopy (FEG-SEM) and X-ray energy dispersive spectroscopy (EDS) analysis (Jeol JSM 7500F) were performed aiming at evaluating the material morphology. The electron beam energy applied was 10 keV. Colour mapping was also performed using the same equipment. The samples were prepared by dropping a CuPh/PC suspension on a silicon plate and drying for 24 hours.

Raman spectroscopy was carried out directly on the powder samples using a Raman spectrometer Witec model Alpha 300R. The experiments were conducted following calibration at 514 nm (green laser) at low power level in the range of 0 to 4000 cm^{-1} after 10 seconds and 10 cycles of exposure.

Transmission electron microscopy (TEM) analysis was conducted using a JEOL JEM-2100 equipment operating at 200 kV. Diluted particle dispersions had been immobilized into carbon-coated copper grids, allowing slowly solvent evaporation at room temperature.

3 Results and discussion

3.1 Morphological and structural characterization

The morphology of the materials PC, CuPh and CuPh/PC (in the ratio 1:4) was evaluated by scanning electron microscopy. The images obtained are depicted in Figure 1.

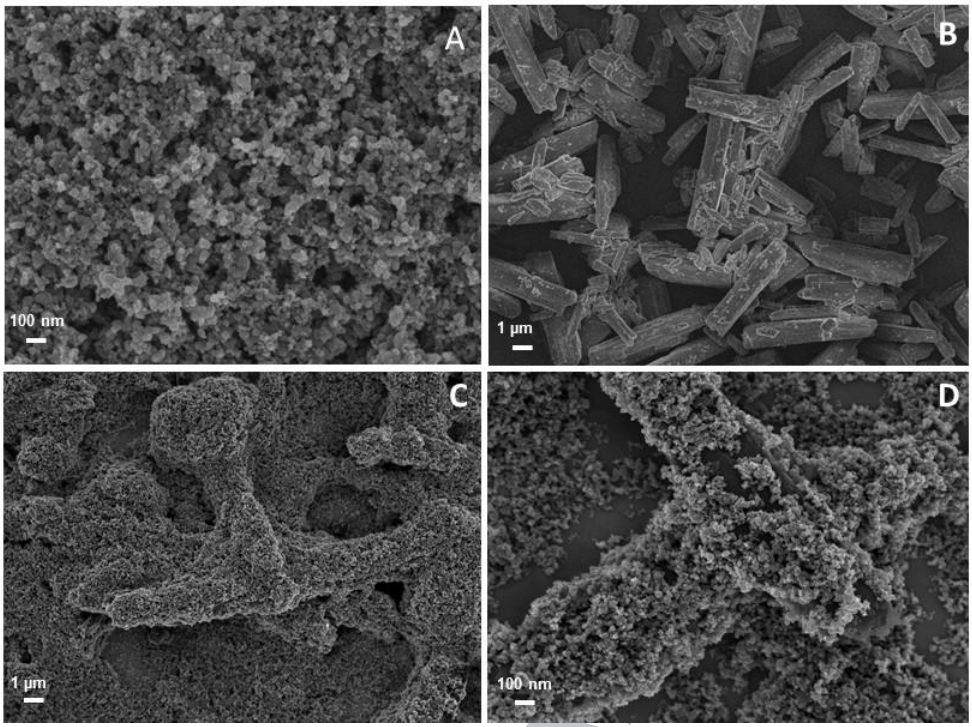

Figure 1: FEG-SEM images obtained for PC (A), CuPh (B) and CuPh/PC 1:4 (wt %) films (C and D) in different magnifications.

Figure 1 (A) shows the image of a nanostructured, homogeneous and highly porous PC film with average particle size of 20 nm. As these particles can aggregate to form agglomerates, the pore size of PC samples can range from microporous (up to 2 nm) to mesoporous (2 to 50 nm).[33] CuPhs film (Figure 1B) exhibits rod-like structures with size of 10 µm. The film obtained by mixing PC and CuPh (CuPh/PC) combined the respective characteristics of the separated materials. In Figures 1C and 1D (with different maginifications), one can clearly observe the CuPh micrometric rods covered by the CB nanoparticles. The presence of micro and mesoporous structures remains after CuPh modification. An increase in surface area is also expected due to size of CuPh. Moreover, the adsorption of the copper phthalocyanine and carbon black materials could be confirmed.

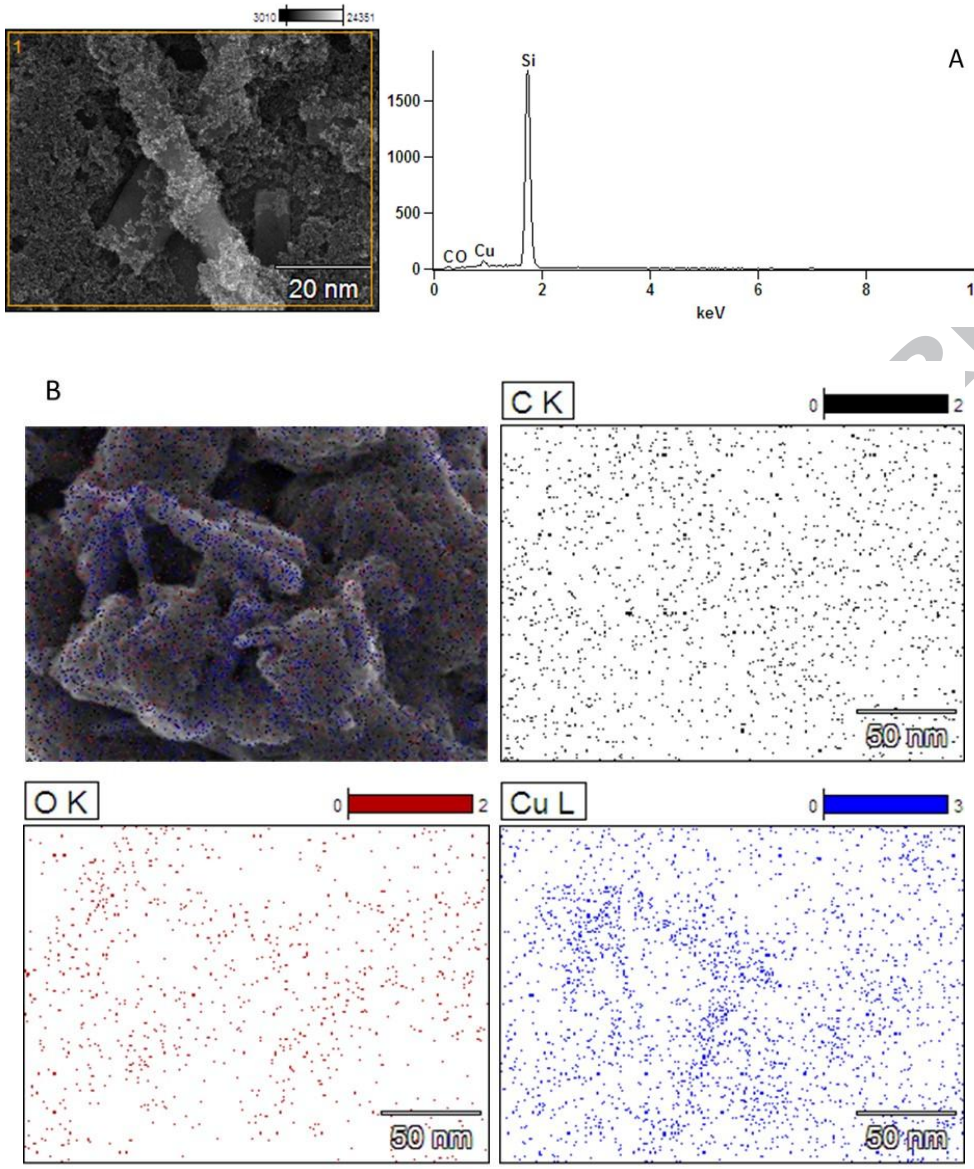

Figure 2: (A) CuPh/PC energy dispersive spectroscopy (EDS) analysis recorded at 10 kV accelerating voltage and 15,000 magnification and (B) colour mapping image of CuPh/PC film 1:4 (wt %).

Energy dispersive spectroscopy measurements (Figure 2A) confirmed the presence of carbon, oxygen, copper and silicon elements of 0.280, 0.527, 0.937 and 1.740 corresponding energies. Si is attributed to the substrate used for characterising the analysis. Literature reports show that PC carbon contains oxygenated groups on its surface. [34] Copper atoms are the metallic centre of the phthalocyanine group. Figure 2B represents the colour mapping image of

the CuPh/PC material. Homogeneous dispersion of carbon and oxygen atoms was observed along the film surface. The presence of copper atoms is more intense on the rods structure.

Through the Raman spectroscopy measurements conducted (Figure 3), Cu-N bond deformation was noted which may be attributed to the phthalocyanine due to the presence of two bands around 232 and 254 cm^{-1}. [35] Grządziel *et al.* (2017) [35] and Beaulieu-Houle *et al.* (2014) [36] reported that the intense band at 593 cm^{-1} can be attributed to CuPc macro-cycle ring while C-N-C and N-C-C bending modes can be assigned to the band at 680 cm^{-1}. The low intensity bands at 1141, 1037 and 833 cm^{-1} can be attributed respectively to pyrrole breathing vibrational mode, C-H bending and C-N stretching. [35] C-N stretching vibration can be associated with the band close to 1344 cm^{-1}. The intense band at 1533 cm^{-1} is assigned to isoindole mode according to Wang et *al.* (2014) [37] and Grządziel *et al. (2017)*. [35] The band at 1448 cm^{-1} was assigned as C_β –C_β, C_β –C_γ –H and C_α –N_β, N_α –C_α –C_β , C–C–H by Basova *et al*. (2009). [38]

The CuPh/PC material exhibited the three of the most intense bands of CuPh at 594, 678 and 1515 cm^{-1}, Figure 3C. The characteristic D (1340 cm^{-1}) and G (1580 cm^{-1}) bands were observed for the PC and CuPh/PC samples, thus confirming the composition of amorphous carbon. [2] The G-band is usually related to sp^2 domains vibrations of graphene or single-crystal graphite. The D-band, on the other hand, is attributed to disorder and imperfection of carbon crystallites. [2] Printex L6 carbon black (Figure 3B) presents the G peak close to 1577 cm^{-1}. This shift in G peak position is characteristic of transition from nanocrystalline graphite to amorphous carbon. [39] This transition also

depends on the relation between intensity of D band and the clustering of the sp^2 phase. This parameter directly influences optical, electrical and mechanical properties of amorphous carbon. [39] The intensity of D band is relatively higher for Printex L6 carbon black when compared to other carbon nanomaterials. This could imply PC L6 presents higher evolution of sp^2 clusters or, in other words, higher ordering of amorphous carbon crystallites. [39] The incorporation of the CuPh has lowered such intensity proving the insertion of sp^2 rings and consequently dropping the degree of imperfection. [39]

Thus, I_D/I_G ratio can be calculated from these results indicating the order/disorder of amorphous carbon. The same ratio of 1.84 was obtained for both PC and CuPh/PC samples, although relatively lower D bands intensities are observed for CuPh/PC material. Reduced intensities indicate the introduction of sp^3 carbon proving successful modification of carbon matrice. Even after the incorporation of CuPh, the CB maintain its properties. Other nanocarbon materials such as pristine carbon nanotubes, [40] functionalized-CNT [41] and graphene [42] present lower I_D/I_G values compared to carbon black. This implies diminished amount of defect sites and terminal groups resulting in higher purity material. [41] The increase of this ratio would also suggest higher sp^3 carbon content probably bonded to oxygenated functional groups at Printex L6 CB structure though not exceeding 20%. [39,43]

A further observation that merits mentioning is that the ratio obtained for PC 6L is relatively lower than the reported values for other carbon black materials such as Vulcan XC72R (2.64) and Vulcan E2000 (2.36). [2] The lower I_D/I_G ratio in PC 6L could be attributed to its relatively smaller number of defects compared to Vulcan suggesting Printex L6 presents higher degree of order than

other carbon black materials. These findings are strong evidences to classify carbon black as a material in transition between nanocrystalline graphite and amorphous carbon. [41] Vulcan resembles more nanocrystalline graphite due to higher I_D/I_G ratio. In contrast, according to the amorphization trajectory and decreased I_D/I_G ratio, [39] Printex L6 properties are more similar to pure amorphous carbon and in less extent to nanocrystalline graphite.

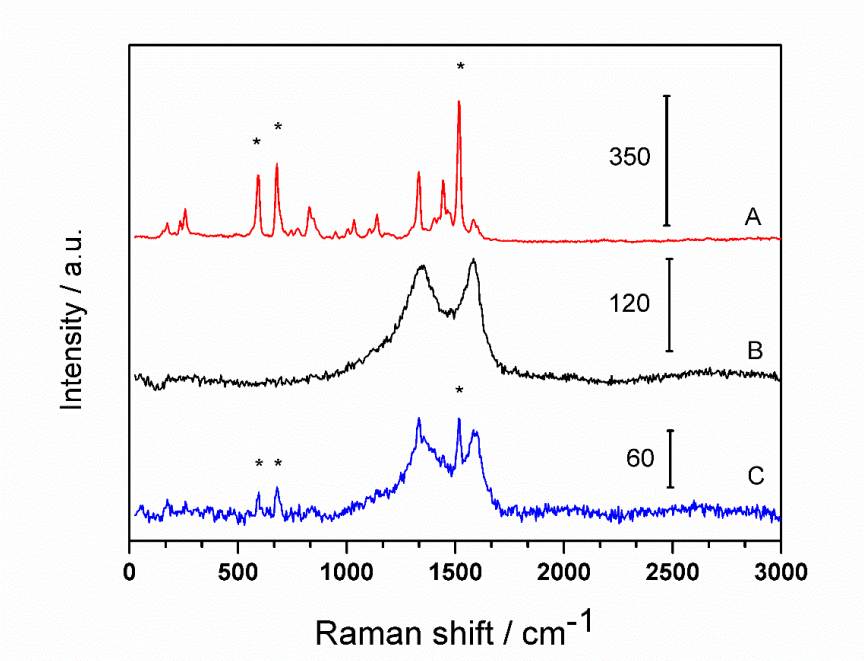

Figure 3: Raman spectra of (A) phthalocyanine, (B) Printex L6 carbon and (C) CuPh/PC 1:4 (wt %) materials.

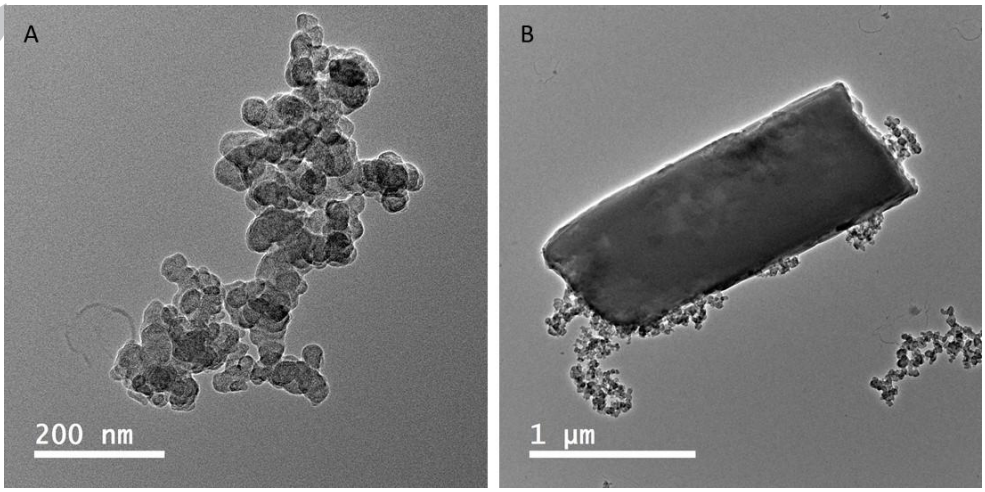

Figure 4: TEM images of (A) Printex L6 carbon and (B) CuPh/PC 1:4 (wt %) materials.

The prepared materials have also been characterised using TEM analysis. The CuPh (Figure 4B) is covered with Printex L6 carbon black (Figure 4A) nanoparticles. These results are in agreement with the scanning electron microscopy results.

3.2 TMP electrochemical behavior

First, the electrochemical behavior of TMP was analysed by cyclic voltammetry in 0.2 mol L^{-1} PBS buffer and under pH of 7.0 for PC/GC, CuPh/GC and CuPh/PC/GC electrodes. TMP electrochemical performance also compared to the bare GC and pure CuPh film. Figure 5A describes the irreversible behavior of TMP confirmed by the presence of an anodic oxidation peak at 1.10 V for both PC and CuPh/PC carbon-based materials, Figure 5Ac and 5Ad respectively. Pure carbon has proven to be massively more conductive compared to pure phthalocyanine (Figure 5A curves c and b respectively). A significant increase in peak current (80 µA) was observed after the modification of carbon black with CuPh. Very low and not well-defined peak current close to 1.2 V was observed for the bare GC (Figure 5Aa) and CuPh/GC (Figure 5Ab) electrodes. The carbon black induces a shift (100 mV) in the direction of less positive potentials when compared to CuPh/GC and GC electrodes. The addition of small amount of copper phthalocyanine to the carbon black has evidently improved material sensitivity towards TMP determination. Xxxx. These results clearly indicate that the combination of PC and CuPh materials produces electrocatalytic effect in addition to contributing towards improving electron transfer on the film surface.

A similar behavior has been reported for CNTs modified with metal-phthalocyanine in which the modified film revealed higher electrochemical response in relation to each single material. [12]

The proportion of phthalocyanine as a carbon modifier was studied in this work. Phthalocyanine/carbon 1:2, 1:4 and 1:6 (wt %) relations were investigated (Figure 5B). The experiments conducted in this work reveal that an excess of phthalocyanine (1:2) can cause a massive reduction of peak current values. This result is in agreement to the nature of CuPh as an organic semiconductor material and the excess of this material would lower conductivity. [14] By diminishing the amount of phthalocyanine in carbon (1:4), anodic peak current significantly improves in relation to pure carbon. And when the amount of phthalocyanine is reduced (1:6), peak current drastically declines. In view of that, subsequent experiments were conducted using CuPh/PC/GC electrode with a ratio of 1:4 CuPh/PC.

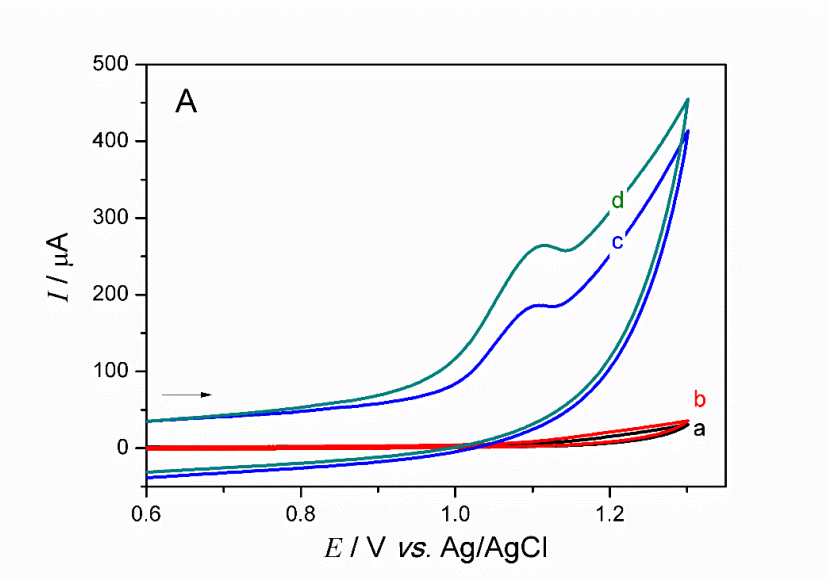

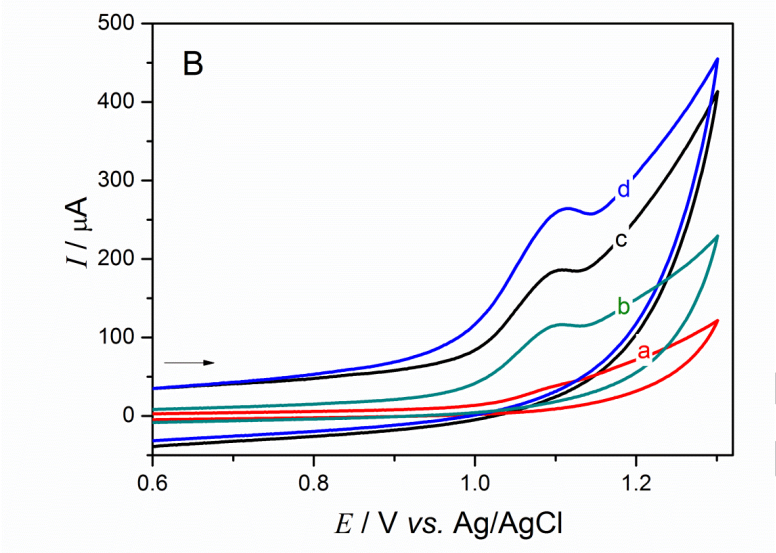

Figure 5: Cyclic voltammograms for 3.0×10^{-4} mol L^{-1} TMP in 0.2 mol L^{-1} phosphate buffer solution at pH 7.0, recorded for (A) GC (a), CuPh/GC (b), PC/GC (c) and CuPh/PC/GC (d). v = 50mV s^{-1}. (B) CVs recorded for pure PC (c) and different proportions of CuPh/PC (wt %) 1:2 (a), 1:6 (b), and 1:4 (d).

Although carbon black is a widely studied catalyst for H_2O_2 electrosynthesis and more recently as electrochemical sensor, some properties of these materials are not well defined. Metallophthalocyanine are electron transfer mediators with great adsorption to carbon nanomaterials. [15,16] Carbon black (CB) is widely known for the superficial sp^2 orbitals and consequently p pure orbitals available for interactions. For this reason, the obtained CuPh/PC electrode could be described as noncovalent hybrid material with strong adsorption through the π-π interactions. These interactions are usually governed by the phthalocyanine planar macrocycle distortion to increase the contact area with carbon surface. This effect is regardless of chemical nature of the central atom over the binding energy. Furthermore, such effect was reported based on the frontier HOMO and LUMO orbitals, spin

density and binding energy studies of CuPh (paramagnetic open-shell) and CNTs. [44] Therefore, when CB and CuPh are combined at an appropriate ratio, there is increased superficial electron availability all over the material causing the synergistic effect. This property, certainly favours electrochemical oxidation reactions and results in improved current responses [12] as observed for the TMP compound. This effect is due to greater electron transfer rate for this process.

The exact interaction between the analytes and the metallophthalocyanine are not always explored in electroanalysis. The literature reports macrocyclic compounds are usually based in the metal atom of the phthalocyanine offering extra adsorption sites to organic compounds. [11,45] Recently, the interactions between the central metal atom and the π-cloud of organic molecules have demonstrated no effect on sensor response. [46] The improved sensor response was attributed to the π-π interactions of periphery substituents the CuPh and the analyte, [46] as the frontier orbitals of CuPh have no metal character.[15,16] Presumably, the increased electrochemical performance for the proposed CuPh/PC/GC sensor is favoured by the π-π interactions of the CuPh/PC film and the aromatic rings of the TMP compound. These stable π system interactions result in faster diffusion of the organic compound across the porous material. [46] In addition, the presence of PC mesoporous structures favors the adsorption of TMP through these channels into PC internal pores. [47] These π-π electrons interactions facilitate electron transfer from the solution/electrode interface through the material until the substrate.

The electrochemical characterization of the modified material in 0.2 mol L^{-1} PBS buffer (pH 7.0) (supplementary material as Figure S1) revealed the presence of two oxidation peaks at 0.85 and 1.10 V and a reduction peak at 0.48 V at the cyclic voltammograms. The oxidation peaks could also be confirmed using SWV technique. The presence of these peaks could be associated to the interaction of copper (II) with phosphate ion (Cu-O) [48], corroborating the idea that the phthalocyanine metal atom would not be interacting with the carbon surface or the TMP but the electrolyte only.

3.2.1 TMP oxidation mechanism

TMP oxidation on CuPh/PC/GC may occur in a manner similar to the mechanism proposed by Rajith, L. *et al* for manganese porphyrin. [11] The overall reaction (Figure 6) occurs by the consumption of 4 electrons and deprotonation of the amino group. [11] The first step involving TMP oxidation pathway is the deprotonation of the NH_2 group followed by the loss of one electron. This step is repeated until the complete oxidation. [11]

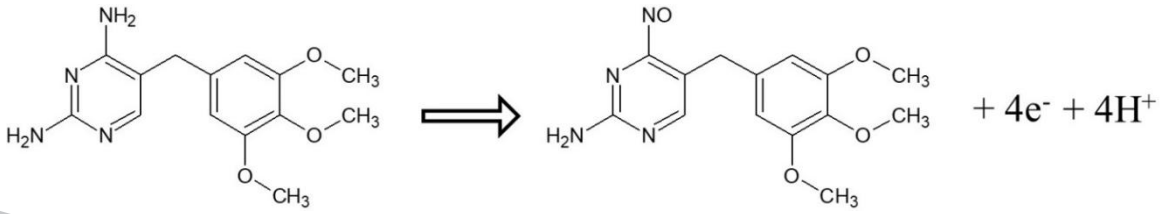

Figure 6: Trimethoprim catalytic oxidation mechanism.

3.2.2 Study of the influence of scan rate and TMP adsorption

Cyclic voltammetry was used to evaluate the effect of scan rate on the TMP electrochemical response on the CuPh/PC/GC electrode (Figure 7). The experiments were performed using 3.0×10^{-4} mol L^{-1} TMP in 0.2 mol L^{-1}

phosphate buffer (pH 7.0) and the scan rate was kept within the range of 5 to 200 mV s^{-1} so as to evaluate TMP oxidation.

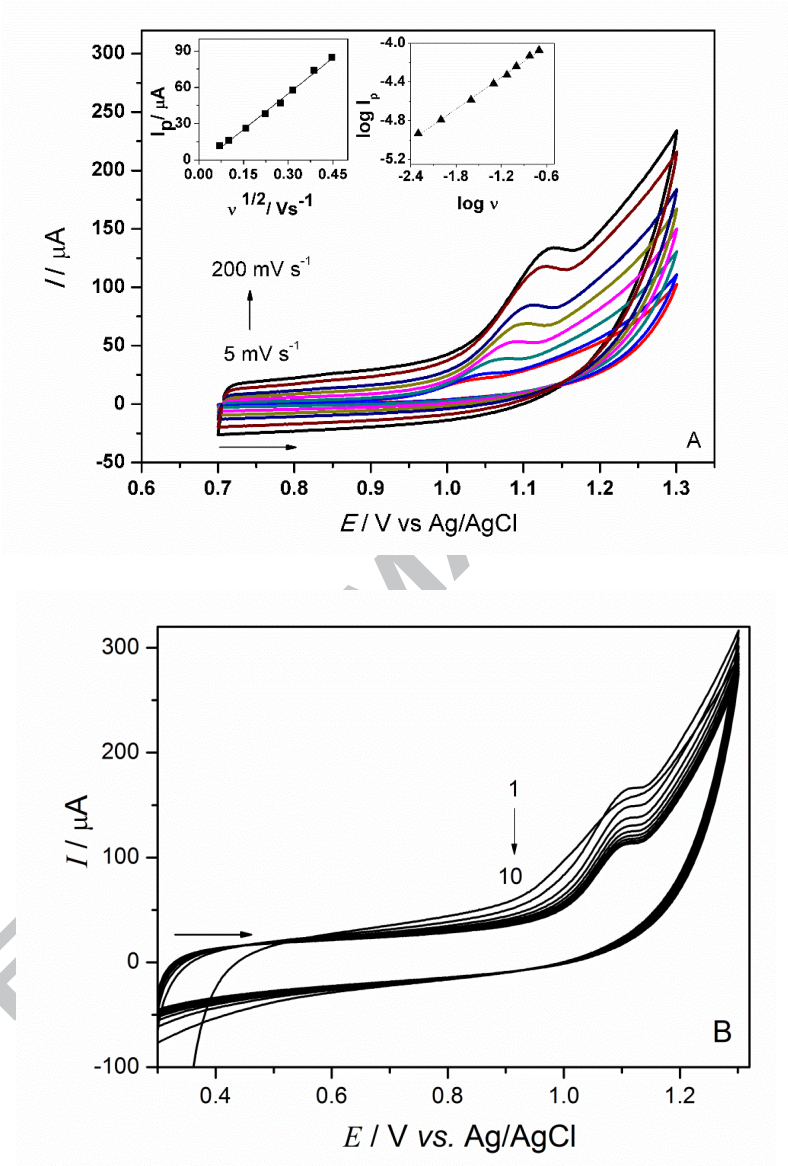

Figure 7: (A) Cyclic voltammograms of CuPh/PC/GC electrode for 3.0×10^{-4} mol L^{-1} TMP in 0.2 mol L^{-1} PBS (pH 7.0) at different scan rates ranging from 5 to 200 mVs^{-1}. Inset: the oxidation peak current vs. square root of the scan rate and the log I_p *vs* log v (scanning range: 0.7 to 1.3 V). (B) 10 successive cyclic voltammograms on CuPh/PC/GC electrode (v = 50 mVs^{-1}).

According to the literature, mass transfer across the electrode surface is associated with the relation between the anodic peak current (I_{ap}) and scan rate (v). Whenever a linear association is obtained from I_{ap} versus $v^{1/2}$, the process is said to be diffusion controlled. Conversely, if there is a linear relationship between I_{ap} and v, the process is found to be adsorption-controlled. [1] In our present study, both adsorption and diffusion of the species on the electrode surface occurs suggesting electrode reactions across the surface progressively change from adsorption to diffusion. [49] The regression equations (1 and 2) are described:

$$I_{ap} = -4.32 \times 10^{-6} + 1.97 \times 10^{-4}\, v;\ (r = 0.995) \qquad \text{Equation (1)}$$

$$I_{ap} = 1.55 \times 10^{-5} + 3.75 \times 10^{-4}\, v;\ (r = 0.969) \qquad \text{Equation (2)}$$

TMP anodic peak current is shifted towards more positive potentials as the scan rate is increased. Figure 7A describes the linear relationship observed between I_{ap} and $v^{1/2}$ ($r = 0.995$) with a slope of 1.97×10^{-4}. The slope is 3.75×10^{-7} for the I_{ap} and v relation ($r = 0.969$). Although linearity is observed for both the square root of the scan rate and the scan rate, diffusion of the TMP species is the dominant effect as indicated by the lower slope of the linear relation. For this reason, diffusion limits the rate of mass transfer on the electrode surface. [49] This observation could also be confirmed considering the linear relationship between the logarithm of the peak current ($\log I_p$) and the logarithm of the scan rate ($\log v$) (Eq. 3) with a slope of 0.54 ($r = 0.997$) [1] (inset Figure 7A).

$$I_{ap} = -3.7 + 0.54\, v;\ (r = 0.997) \qquad \text{Equation (3)}$$

The adsorptive feature of TMP was studied using cyclic voltammetry (Figure 7B). Following 10 successive scans, the TMP oxidation process at 1.1 V

was found to decrease significantly as the number of scans increased from 1 to 10. It is likely that the TMP oxidation product (Figure 7) forms a film on the electrode surface, hampering diffusion of species to the active sites and consequently lowering the peak current. [50] In light of that, the effects of pre-concentration potential and time on TMP determination were studied using SWV in the range of 0.6 to 1.3 V (data not shown). Initially, the time was set at 60 s and the potential was studied at -0.2; 0.0; +0.2; +0.4; +0.6, and +0.9 V. Relatively higher peak current and peak definition were obtained at +0.6 V. An increase of 0.35 A was observed in the peak current when the potential was applied for 120 s. Regarding longer periods of time, the peak current was found to decrease given an increase in time. The peak definition and peak current were both found to decline at shorter periods of time.

TMP adsorption process in massively influenced by the solution pH. Once again, the presence of oxygenated surface group affects this process. Maximum TMP peak current had been obtained at pH 7.0; for lower and greater values, peak current massively decreases (data not shown). This trend is associated to the adsorption of TMP molecule in the carbon black surface. Similar trend has been reported. [47] This process is known as proton exchange mechanism thus mediated by H^+ release to solution.

Prior to the electrochemical oxidation of TMP, firstly pore diffusion and chemical interactions occurs. The presence of CB mesopores facilitates diffusion of species to the internal pores. The enhanced catalytic activity of carbon black materials is commonly attributed to the superficial oxygenated groups. These groups are responsible for altering the acid-base character and the electron donor/acceptor properties of carbon materials. [47] Carboxylic acid

and lactonic groups can act as π-electron-acceptors and promote strong interaction with aromatic rings of TMP due to π–π electron donor-acceptor interactions. [47] Besides, strong hydrogen bonds interaction can be formed between these oxygen rich groups and the $–CH_3$ (amino) and/or $–OCH_3$ (methoxy) substituents of TMP. [47] These π–π electron interactions can also be established with the aromatic rings present of the CuPh ligand.

Considering TMP pka (pka_1= 3.2 and pKa_2= 6.7) [51] and the solution pH (7.0), one group of the molecule is deprotonated and the other partially protonated/deprotonated. Thus, an electrostatic interaction is possible between the TMP negatively charged with the aromatic system of phthalocyanine and carbon oxygen rich groups.

3.3 Analytical performance

TMP determination was carried out via optimized analytical method using square-wave adsorptive anodic stripping voltammetry (SWAdASV) technique and CuPh/PC/GC electrode. The pre-concentration step at +0.6 V for 120 s was performed prior to all studied conditions. The parameters including amplitude (a), frequency (f) and scan increment (ΔE) were optimized in the range of 5 - 100 (mV), 10 – 60 (Hz) and 1 – 10 (mV) respectively for TMP determination. The values were selected based on the magnitude and shape of the analytic signal, repeatability, accuracy and baseline stability. [1] The parameters and their respective values are shown in Table 1 below.

Table 1: SWV optimized parameters for CuPh/PC/GC

Parameters	studied range	selected value
Amplitude (mV)	5 - 100	40
Frequency (Hz)	10 - 60	10
Step potential (mV)	1 - 10	5

Figure 8 shows SWV curves obtained for varying concentrations of TMP in 0.2 mol L^{-1} PBS under pH of 7.0. Results show the anodic peak current was directly proportional to the TMP concentration in two different ranges consisting of 0.4 to 1.1 μmol L^{-1} and 1.5 to 6.0 μmol L^{-1} (r = 0.994 and 0.986) respectively. The linear regression equations obtained from the analytical curves are I_{p1} = 8.89×10^{-7} + 5.82 [TMP] and I_{p2} = 9.09×10^{-6} + 0.79 [TMP] ($\times10^{-6}$ mol L^{-1}). The calculated detection limit (LOD) was 6.70×10^{-7} and 4.93×10^{-6} mol L^{-1} for the first and second linear regions respectively (n = 3).

The presence of two linear segments in the determination of TMP suggest a mixed mass transportation system. The first linear region presents a higher slope as a result of strong adsorption process of the analyte on the CuPh/PC/GC electrode surface. The presence of a second linear region with a lower slope, indicates the beginning of a diffusion process on the previously formed monolayer at the material surface. Besides, in determinations of this nature, both linear ranges can be used to TMP quantification. [52,53]

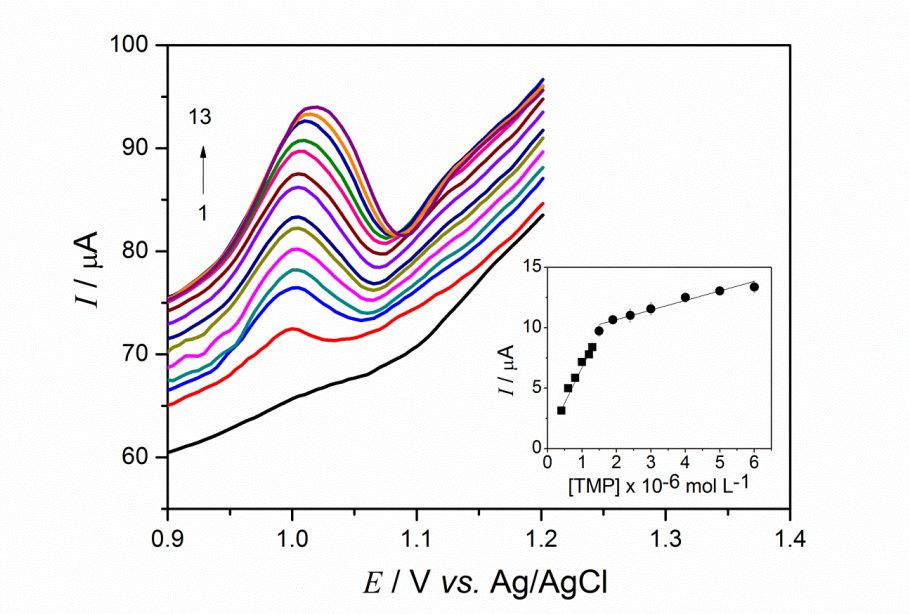

Figure 8: Square wave voltammograms for CuPh/PC/GC sensor with the optimized parameters. The different TMP concentrations ranged from blank to 0.4 (1), 0.6 (2), 0.8 (3), 1.0 (4), 1.2 (5), 1.3 (6), 1.5 (7), 1.9 (8), 2.4 (9), 3.0 (10), 4.0 (11), 5.0 (12) and 6.0 × 10^{-6} mol L^{-1} (13). Inset: linear dependence of the anodic peak current *vs.* TMP concentrations (0.4 to 1.1 µmol L^{-1} (squares) and 1.5 to 6.0 µmol L^{-1} (circles)).

Previous results reported in literature using electroanalytical methods for TMP determination had been compared to the results obtained in this work (see Table S1 in the supplementary data). CuPh/PC has a low detection limit similar to the ones reported for BDD [54] and MIP-graphene-GC. [18] Although CNTs [55,56] presented even lower LOD, both CNTs [56] and BDD [19,54] materials are more expensive than carbon black.

3.4 TMP determination in natural water samples

The application of the developed CuPh/PC/GC sensor was conducted by the determination of TMP in natural water using the optimized SWV methodology. The river water samples were spiked with two fortification levels of 5.0 and 10.0×10^{-6} mol L^{-1}. The results obtained in terms of recovery percentage are presented in Table 2. CuPh/PC/GC sensor has essentially proven to be reliable for the determination of pharmaceutical compounds. Excellent recoveries of 97.4 and 99.6% demonstrate undoubtedly that the sensor can be applied successfully towards TMP determination even in the presence of a complex matrix. These results reinforce the application potential and suitability of CuPh/PC/GC sensor in environmental monitoring analysis. Environmental samples analysis is highly demanded. [57] as well as the monitoring at the end point of industrial level wastewater. [24]

Table 2: TMP determination in water sample by SWV.

Sample*	Added/µmol L^{-1}	Found/µmol L^{-1}	% Recovery	RSD
River Water	5.0	4.87	97.4	0.9703
	10.0	9.96	99.6	0.9712

*(n = 3)

3.5 Interfering agents, Reproducibility and stability

The determination of 3.0×10^{-4} mol L^{-1} of TMP was performed in the presence of interfering agents for the CuPh/PC/GC sensor. Inorganic and organic compounds were added to 0.2 mol L^{-1} PBS buffer solution (pH 7.0). The organic interfering agents were selected taking into account the possible substances present in river water such as dyes, endocrine disruptor and other

pharmaceutical compounds. The ratios of TMP to interfering agents were 1:100 and 1:50 for inorganic and organic agents respectively. The ions Na^+, K^+, Cl^-, and SO_4^{2-} (93.2, 99.6, 99.6 and 102.8%) were found to present no interference in TMP determination. By contrast, propylparaben, alizarin, dipyrone and paracetamol enabled TMP detection with great recoveries of 90.4, 97.2, 96.4 and 93.3% respectively.

Reproducibility of the CuPh/PC/GC electrode was investigated using the previously optimized SWV method. Three successive determinations were carried out and the relative standard deviation (RSD) obtained was 5.4 %, which is clear evidence that the sensor is, indeed, reproducible. Furthermore, the CuPh/PC/GC electrode stability was studied considering films prepared at 1, 15 and 30 days prior to measurements. The material presented a stable anodic peak current. The Ipa values of 103.9 and 94.5% obtained suggest the material exhibits great stability as an electrochemical sensor when stored in air and at room temperature for a long time. [58]

4 Conclusion

The modification of Printex L6 carbon black nanospheres with copper (II) phthalocyanine has proven to be effective in the synthesis of a new sensing material. There is strong adsorption of CuPh in the PC surface due to the π-π interactions. The combination of CB and CuPh materials proved electrocatalytic effect towards TMP determination. The cyclic voltammetric results for the CuPh/PC/GC sensor showed an increase in the analytical response and improvement in the electron transfer kinetics for TMP oxidation compared to the bare GC electrode. The proportion of CuPh in PC demonstrated to have a

massive impact on the electrochemical performance of the material since relatively larger amounts of phthalocyanine contributed towards a decline in the TMP analytical signal. Scan rate studies demonstrated TMP mass transfer across the surface progressively changes from adsorption to diffusion at carbon/CuPh surface. The proposed CuPh/PC/GC sensor was applied to TMP determination using square-wave adsorptive anodic stripping voltammetry (SWAdASV). Two linear ranges of 0.4 to 1.1 μmol L^{-1} and 1.5 to 6.0 μmol L^{-1} were obtained with limit of detection of 6.7×10^{-7} mol L^{-1}. Both curves can be used at TMP quantification. Based on the results obtained, the proposed material has, in effect, proven to have excellent stability and repeatability. The successful testing of the material in natural water shows its great potential for application in water quality control.

5 Acknowledgments

The authors would like to express their sincerest gratitude and indebtedness to the Brazilian Research Funding Agencies including grants #2014/11861-0, #2014/50945-4, #2016/01937-4 and #2016/08760-2, São Paulo Research Foundation (FAPESP), Capes and CNPq for the financial support provided during the course of this work. Our thanks also go to LMA-LIEC in Araraquara for providing the FEG-SEM facilities. Thanks for Dr. Daniel F. Segura for art work support.

6 References

[1] L.P. Silva, F.C. Vicentini, B.C. Lourencao, G.G. Oliveira, M.R. V. Lanza, O. Fatibello-Filho, A new sensor architecture based on carbon Printex 6L to the electrochemical determination of ranitidine, J. Solid State

Electrochem. 20 (2016) 2395–2402. doi:10.1007/s10008-016-3143-5.

[2] F.C. Vicentini, A.E. Ravanini, L.C.S. Figueiredo-Filho, J. Iniesta, C.E. Banks, O. Fatibello-Filho, Imparting improvements in electrochemical sensors: Evaluation of different carbon blacks that give rise to significant improvement in the performance of electroanalytical sensing platforms, Electrochim. Acta. 157 (2015) 125–133. doi:10.1016/j.electacta.2014.11.204.

[3] Y. Zhou, L. Tang, G. Zeng, J. Chen, Y. Cai, Y. Zhang, G. Yang, Y. Liu, C. Zhang, W. Tang, Mesoporous carbon nitride based biosensor for highly sensitive and selective analysis of phenol and catechol in compost bioremediation, Biosens. Bioelectron. 61 (2014) 519–525. doi:10.1016/j.bios.2014.05.063.

[4] C.M. Long, M.A. Nascarella, P.A. Valberg, Carbon black vs. black carbon and other airborne materials containing elemental carbon: Physical and chemical distinctions, Environ. Pollut. 181 (2013) 271–286. doi:10.1016/j.envpol.2013.06.009.

[5] F. Arduini, F. DiNardo, A. Amine, L. Micheli, G. Palleschi, D. Moscone, Carbon Black-Modified Screen-Printed Electrodes as Electroanalytical Tools, Electroanalysis. 24 (2012) 743–751. doi:10.1002/elan.201100561.

[6] C. Takei, K. Kakinuma, K. Kawashima, K. Tashiro, M. Watanabe, M. Uchida, Load cycle durability of a graphitized carbon black-supported platinum catalyst in polymer electrolyte fuel cell cathodes, J. Power Sources. 324 (2016) 729–737. doi:10.1016/j.jpowsour.2016.05.117.

[7] H. Yang, Y. Qiu, X. Guo, Lead oxide/carbon black composites prepared with a new pyrolysis-pickling method and their effects on the high-rate

partial-state-of-charge performance of lead-acid batteries, Electrochim. Acta. 235 (2017) 409–421. doi:10.1016/j.electacta.2017.03.138.

[8] M.H.M.T. Assumpção, R.F.B. De Souza, D.C. Rascio, J.C.M. Silva, M.L. Calegaro, I. Gaubeur, T.R.L.C. Paixão, P. Hammer, M.R. V Lanza, M.C. Santos, A comparative study of the electrogeneration of hydrogen peroxide using Vulcan and Printex carbon supports, Carbon N. Y. 49 (2011) 2842–2851. doi:10.1016/j.carbon.2011.03.014.

[9] J.F. Carneiro, R.S. Rocha, P. Hammer, R. Bertazzoli, M.R.V. Lanza, Hydrogen peroxide electrogeneration in gas diffusion electrode nanostructured with Ta2O5, Appl. Catal. A Gen. 517 (2016) 161–167. doi:10.1016/j.apcata.2016.03.013.

[10] W.R.P. Barros, S.A. Alves, P.C. Franco, J.R. Steter, R.S. Rocha, M.R. V. Lanza, Electrochemical Degradation of Tartrazine Dye in Aqueous Solution Using a Modified Gas Diffusion Electrode, J. Electrochem. Soc. 161 (2014) H438–H442. doi:10.1149/2.015409jes.

[11] L. Rajith, A.K. Jissy, K.G. Kumar, A. Datta, Mechanistic Study for the Facile Oxidation of Trimethoprim on a Manganese Porphyrin Incorporated Glassy Carbon Electrode, J. Phys. Chem. C. 115 (2011) 21858–21864. doi:10.1021/jp208027s.

[12] X. Zuo, H. Zhang, N. Li, An electrochemical biosensor for determination of ascorbic acid by cobalt (II) phthalocyanine-multi-walled carbon nanotubes modified glassy carbon electrode, Sensors Actuators, B Chem. 161 (2012) 1074–1079. doi:10.1016/j.snb.2011.12.013.

[13] S. Eyele-Mezui, P. Vialat, C. Higy, R. Bourzami, C. Leuvrey, N. Parizel, P. Turek, P. Rabu, G. Rogez, C. Mousty, Electrocatalytic Properties of Metal

Phthalocyanine Tetrasulfonate Intercalated in Metal Layered Simple Hydroxides (Metal: Co, Cu, and Zn), J. Phys. Chem. C. 119 (2015) 13335–13342. doi:10.1021/acs.jpcc.5b02985.

[14] N.G. Mphuthi, A.S. Adekunle, O.E. Fayemi, Phthalocyanine Doped Metal Oxide Nanoparticles on Multiwalled Carbon Nanotubes Platform for the detection of Dopamine, Nat. Publ. Gr. (2017) 1–23. doi:10.1038/srep43181.

[15] J.H. Zagal, S. Griveau, K.I. Ozoemena, T. Nyokong, F. Bedioui, Carbon Nanotubes, Phthalocyanines and Porphyrins: Attractive Hybrid Materials for Electrocatalysis and Electroanalysis, J. Nanosci. Nanotechnol. 9 (2009) 2201–2214. doi:10.1166/jnn.2009.SE15.

[16] J.H. Zagal, S. Griveau, M. Santander-Nelli, S.G. Granados, F. Bedioui, Carbon nanotubes and metalloporphyrins and metallophthalocyanines-based materials for electroanalysis, J. Porphyr. Phthalocyanines. 16 (2012) 713–740. doi:10.1142/S1088424612300054.

[17] Y. Zhang, A. Wang, X. Tian, Z. Wen, H. Lv, D. Li, J. Li, Efficient mineralization of the antibiotic trimethoprim by solar assisted photoelectro-Fenton process driven by a photovoltaic cell, J. Hazard. Mater. 318 (2016) 319–328. doi:10.1016/j.jhazmat.2016.07.021.

[18] H. da Silva, J.G. Pacheco, J. MCS Magalhães, S. Viswanathan, C. Delerue-Matos, MIP-graphene-modified glassy carbon electrode for the determination of trimethoprim, Biosens. Bioelectron. 52 (2014) 56–61. doi:10.1016/j.bios.2013.08.035.

[19] L.S. Andrade, R.C. Rocha-Filho, Q.B. Cass, O. Fatibello-Filho, Simultaneous Differential Pulse Voltammetric Determination of

Sulfamethoxazole and Trimethoprim on a Boron-Doped Diamond Electrode, Electroanalysis. 21 (2009) 1475–1480. doi:10.1002/elan.200804551.

[20] U. Rashid, W. Ahmad, S.F. Hassan, N.A. Qureshi, B. Niaz, B. Muhammad, S. Imdad, M. Sajid, Design, synthesis, antibacterial activity and docking study of some new trimethoprim derivatives, Bioorg. Med. Chem. Lett. 26 (2016) 5749–5753. doi:10.1016/j.bmcl.2016.10.051.

[21] Y. Zhou, X. Liu, Y. Xiang, P. Wang, J. Zhang, F. Zhang, J. Wei, L. Luo, M. Lei, L. Tang, Modification of biochar derived from sawdust and its application in removal of tetracycline and copper from aqueous solution: Adsorption mechanism and modelling, Bioresour. Technol. 245 (2017) 266–273. doi:10.1016/j.biortech.2017.08.178.

[22] L.F. Sgobbi, C.A. Razzino, S.A.S. Machado, A disposable electrochemical sensor for simultaneous detection of sulfamethoxazole and trimethoprim antibiotics in urine based on multiwalled nanotubes decorated with Prussian blue nanocubes modified screen-printed electrode, Electrochim. Acta. 191 (2016) 1010–1017. doi:10.1016/j.electacta.2015.11.151.

[23] B. Kolar, L. Arnuš, B. Jeretin, A. Gutmaher, D. Drobne, M.K. Durjava, The toxic effect of oxytetracycline and trimethoprim in the aquatic environment, Chemosphere. 115 (2014) 75–80. doi:10.1016/j.chemosphere.2014.02.049.

[24] X. Liu, Y. Zhou, J. Zhang, L. Luo, Y. Yang, H. Huang, H. Peng, L. Tang, Y. Mu, Insight into electro-Fenton and photo-Fenton for the degradation of antibiotics: Mechanism study and research gaps, Chem. Eng. J. 347

(2018) 379–397. doi:10.1016/j.cej.2018.04.142.

[25] Y.-J. Yang, X.-W. Liu, B. Li, S.-H. Li, X.-J. Kong, Z. Qin, J.-Y. Li, Simultaneous determination of diaveridine, trimethoprim and ormetoprim in feed using high performance liquid chromatography tandem mass spectrometry, Food Chem. 212 (2016) 358–366. doi:10.1016/j.foodchem.2016.05.184.

[26] L.S. Andrade, M.C. de Moraes, R.C. Rocha-Filho, O. Fatibello-Filho, Q.B. Cass, A multidimensional high performance liquid chromatography method coupled with amperometric detection using a boron-doped diamond electrode for the simultaneous determination of sulfamethoxazole and trimethoprim in bovine milk., Anal. Chim. Acta. 654 (2009) 127–32. doi:10.1016/j.aca.2009.09.035.

[27] L. Liu, Q. Wan, X. Xu, S. Duan, C. Yang, Combination of micelle collapse and field-amplified sample stacking in capillary electrophoresis for determination of trimethoprim and sulfamethoxazole in animal-originated foodstuffs, Food Chem. 219 (2017) 7–12. doi:10.1016/j.foodchem.2016.09.118.

[28] O.A. Adegoke, C.P. Babalola, O.A. Kotila, O. Obuebhor, Simultaneous spectrophotometric determination of trimethoprim and sulphamethoxazole following charge-transfer complexation with chloranilic acid, Arab. J. Chem. (2014). doi:10.1016/j.arabjc.2014.05.022.

[29] J. Heinze, Cyclic Voltammetry—“Electrochemical Spectroscopy”. New Analytical Methods(25), Angew. Chemie Int. Ed. English. 23 (1984) 831–847. doi:10.1002/anie.198408313.

[30] X. Wang, J. Liu, R. Qu, Z. Wang, Q. Huang, The laccase-like reactivity of

manganese oxide nanomaterials for pollutant conversion: rate analysis and cyclic voltammetry, Sci. Rep. 7 (2017) 7756. doi:10.1038/s41598-017-07913-2.

[31] S.G. Li, W.T. Xue, H. Zhang, Voltammetric behavior and determination of tocopherol in vegetable oils at a polypyrrole modified electrode, Electroanalysis. 18 (2006) 2337–2342. doi:10.1002/elan.200603663.

[32] R.M. Reis, R.B. Valim, R.S. Rocha, A.S. Lima, P.S. Castro, M. Bertotti, M.R. V Lanza, The use of copper and cobalt phthalocyanines as electrocatalysts for the oxygen reduction reaction in acid medium, Electrochim. Acta. 139 (2014) 1–6. doi:10.1016/j.electacta.2014.07.003.

[33] J. Rouquerol, D. Avnir, C.W. Fairbridge, D.H. Everett, J.M. Haynes, N. Pernicone, J.D.F. Ramsay, K.S.W. Sing, K.K. Unger, Recommendations for the characterization of porous solids (Technical Report), Pure Appl. Chem. 66 (1994) 1739–1758. doi:10.1351/pac199466081739.

[34] E. Yeager, Dioxygen electrocatalysis: mechanisms in relation to catalyst structure, J. Mol. Catal. 38 (1986) 5–25. doi:10.1016/0304-5102(86)87045-6.

[35] L. Grządziel, M. Krzywiecki, G. Genchev, A. Erbe, Effect of order and disorder on degradation processes of copper phthalocyanine nanolayers, Synth. Met. 223 (2017) 199–204. doi:10.1016/j.synthmet.2016.11.024.

[36] G. Beaulieu-Houle, D.F.R. Gilson, I.S. Butler, Pressure-tuning micro-Raman spectra of artists' pigments: α- and β-copper phthalocyanine polymorphs, Spectrochim. Acta - Part A Mol. Biomol. Spectrosc. 117 (2014) 61–64. doi:10.1016/j.saa.2013.07.017.

[37] X. Wang, J. Zheng, K. Qiao, J. Qu, C. Cao, Studies on structure and

Raman spectroscopy of Ni-doped copper phthalocyanine thin films, Appl. Surf. Sci. 297 (2014) 188–194. doi:10.1016/j.apsusc.2014.01.122.

[38] T. V. Basova, V.G. Kiselev, B.E. Schuster, H. Peisert, T. Chass??, Experimental and theoretical investigation of vibrational spectra of copper phthalocyanine: Polarized single-crystal Raman spectra, isotope effect and DFT calculations, J. Raman Spectrosc. 40 (2009) 2080–2087. doi:10.1002/jrs.2375.

[39] A.C. Ferrari, J. Robertson, Interpretation of Raman spectra of disordered and amorphous carbon, Phys. Rev. B. 61 (2000) 14095–14107. doi:10.1103/PhysRevB.61.14095.

[40] S.P. Kim, H.C. Choi, Reusable hydrazine amperometric sensor based on Nafion ® -coated TiO2 – carbon nanotube modified electrode, Sensors Actuators B. Chem. 207 (2015) 424–429. doi:10.1016/j.snb.2014.10.029.

[41] K.K. Reddy, M. Satyanarayana, K.Y. Goud, K. V. Gobi, H. Kim, Carbon nanotube ensembled hybrid nanocomposite electrode for direct electrochemical detection of epinephrine in pharmaceutical tablets and urine, Mater. Sci. Eng. C. 79 (2017) 93–99. doi:10.1016/j.msec.2017.05.012.

[42] T.A. Silva, H. Zanin, E. Saito, R.A. Medeiros, F.C. Vicentini, E.J. Corat, O. Fatibello-Filho, Electrochemical behaviour of vertically aligned carbon nanotubes and graphene oxide nanocomposite as electrode material, Electrochim. Acta. 119 (2014) 114–119. doi:10.1016/j.electacta.2013.12.024.

[43] F.C. Moraes, R.G. Freitas, R. Pereira, L.F. Gorup, A. Cuesta, E.C. Pereira, Coupled electronic and morphologic changes in graphene oxide

upon electrochemical reduction, Carbon N. Y. 91 (2015) 11–19. doi:10.1016/j.carbon.2015.04.038.

[44] V.A. Basiuk, L.J. Flores-Sánchez, V. Meza-Laguna, J.O. Flores-Flores, L. Bucio-Galindo, I. Puente-Lee, E. V. Basiuk, Noncovalent functionalization of pristine CVD single-walled carbon nanotubes with 3d metal(II) phthalocyanines by adsorption from the gas phase, Appl. Surf. Sci. 436 (2018) 1123–1133. doi:10.1016/j.apsusc.2017.12.122.

[45] F.C. Moraes, L.H. Mascaro, S.A.S. Machado, C.M.A. Brett, Direct Electrochemical Determination of Glyphosate at Copper Phthalocyanine/Multiwalled Carbon Nanotube Film Electrodes, Electroanalysis. 22 (2010) 1586–1591. doi:10.1002/elan.200900614.

[46] A. Kumar, J. Brunet, C. Varenne, A. Ndiaye, A. Pauly, Phthalocyanines based QCM sensors for aromatic hydrocarbons monitoring: Role of metal atoms and substituents on response to toluene, Sensors Actuators, B Chem. 230 (2016) 320–329. doi:10.1016/j.snb.2016.02.032.

[47] H. Liu, J. Zhang, H.H. Ngo, W. Guo, H. Wu, Z. Guo, C. Cheng, C. Zhang, Effect on physical and chemical characteristics of activated carbon on adsorption of trimethoprim: Mechanisms study, RSC Adv. 5 (2015) 85187–85195. doi:10.1039/c5ra17968h.

[48] N.A. Odewunmi, A.-N. Kawde, M. Ibrahim, Electrochemically Inspired Copper(II) Complex on Disposable Graphite Pencil Electrode for Effective Simultaneous Detection of Hypoxanthine, Xanthine, and Uric acid, Electroanalysis. (2018) 1–11. doi:10.1002/elan.201800397.

[49] H. Wang, S. Zhang, S. Li, J. Qu, Electrochemical sensor based on palladium-reduced graphene oxide modified with gold nanoparticles for

simultaneous determination of acetaminophen and 4-aminophenol, Talanta. 178 (2018) 188–194. doi:10.1016/j.talanta.2017.09.021.

[50] F.C. Moraes, I. Cesarino, V. Cesarino, L.H. Mascaro, S.A.S. Machado, Carbon nanotubes modified with antimony nanoparticles: A novel material for electrochemical sensing, Electrochim. Acta. 85 (2012) 560–565. doi:10.1016/j.electacta.2012.08.123.

[51] A. Molinari, E. Sarti, N. Marchetti, L. Pasti, Degradation of emerging concern contaminants in water by heterogeneous photocatalysis with Na4W10O32, Appl. Catal. B Environ. 203 (2017) 9–17. doi:10.1016/j.apcatb.2016.09.031.

[52] Y. Fan, K.J. Huang, D.J. Niu, C.P. Yang, Q.S. Jing, TiO2-graphene nanocomposite for electrochemical sensing of adenine and guanine, Electrochim. Acta. 56 (2011) 4685–4690. doi:10.1016/j.electacta.2011.02.114.

[53] J.-M. Zen, M.-R. Chang, G. Ilangovan, Simultaneous determination of guanine and adenine contents in DNA, RNA and synthetic oligonucleotides using a chemically modified electrode, Analyst. 124 (1999) 679–684. doi:10.1039/a900532c.

[54] P.F. Pereira, W.P. Da Silva, R.A.A. Munoz, E.M. Richter, A simple and fast batch injection analysis method for simultaneous determination of phenazopyridine, sulfamethoxazole, and trimethoprim on boron-doped diamond electrode, J. Electroanal. Chem. 766 (2016) 87–93. doi:10.1016/j.jelechem.2016.01.034.

[55] L.F. Sgobbi, C.A. Razzino, S.A.S. Machado, A disposable electrochemical sensor for simultaneous detection of sulfamethoxazole

and trimethoprim antibiotics in urine based on multiwalled nanotubes decorated with Prussian blue nanocubes modified screen-printed electrode, Electrochim. Acta. 191 (2016) 1010–1017. doi:10.1016/j.electacta.2015.11.151.

[56] I. Cesarino, V. Cesarino, M.R.V. Lanza, Carbon nanotubes modified with antimony nanoparticles in a paraffin composite electrode: Simultaneous determination of sulfamethoxazole and trimethoprim, Sensors Actuators B Chem. 188 (2013) 1293–1299. doi:10.1016/j.snb.2013.08.047.

[57] A. Hayat, J.L. Marty, Disposable screen printed electrochemical sensors: Tools for environmental monitoring, Sensors (Switzerland). 14 (2014) 10432–10453. doi:10.3390/s140610432.

[58] L.A. Goulart, L.H. Mascaro, GC electrode modified with carbon nanotubes and NiO for the simultaneous determination of bisphenol A, hydroquinone and catechol, Electrochim. Acta. 196 (2016) 48–55. doi:10.1016/j.electacta.2016.02.174.

CuPh/PC/GC

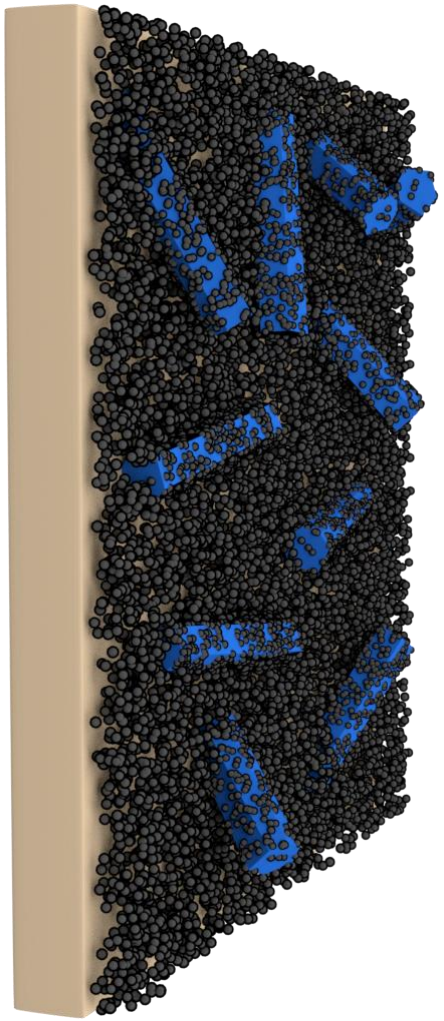

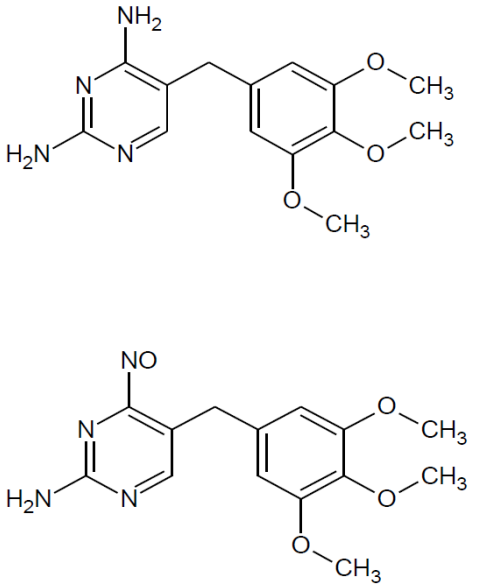
NH2
N
H2N
N
O
CH3
CH3
O
O
CH3
-4e-
NO
N
H2N
N
O
CH3
CH3
O
O
CH3

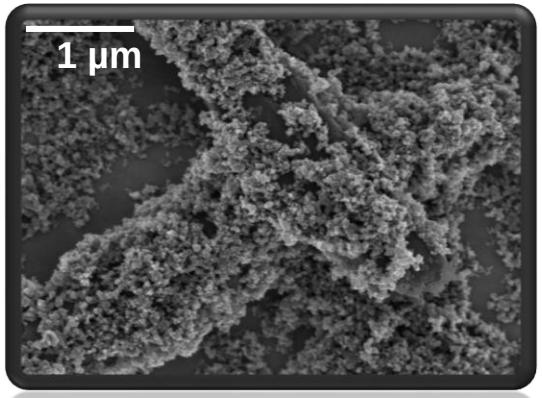
1 µm

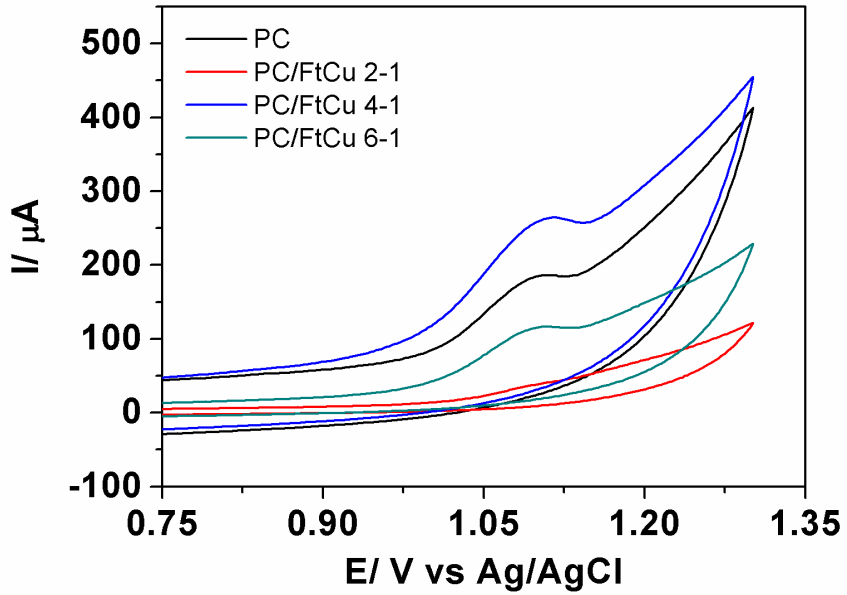
PC
PC/FtCu 2-1
PC/FtCu 4-1
PC/FtCu 6-1
I/ µA
500
400
300
200
100
0
-100
0.75
0.90
1.05
1.20
1.35
E/ V vs Ag/AgCl

Highlights

- Carbon black Printex L6 (PC) was used as cheaper and stable alternative platform for electrochemical sensors development than other carbon nanomaterials.
- Copper phthalocyanine modification resulted in noncovalent hybrid material with strong adsorption to carbon black due to π-π interactions.
- The π-π interactions inside the CuPh/PC and at electrode/electrolyte interface increased sensing response due to faster electron transfer.
- Trimethoprim has been detected in a wide linear range comprised of two linear regions. showing the mixed mass transport